

See discussions, stats, and author profiles for this publication at: <https://www.researchgate.net/publication/279305075>

Rapid Endolysosomal Escape and Controlled Intracellular Trafficking of Cell Surface Mimetic Quantum-Dots-Anchored Peptides and Glycopeptides

ARTICLE *in* ACS CHEMICAL BIOLOGY · JUNE 2015

Impact Factor: 5.33 · DOI: 10.1021/acscchembio.5b00434 · Source: PubMed

CITATION

1

READS

28

5 AUTHORS, INCLUDING:



[Roger Salvacion Tan](#)

Medicinal Chemistry Pharmaceuticals Co., Ltd.

5 PUBLICATIONS 2 CITATIONS

[SEE PROFILE](#)



[Maho Amano](#)

Hokkaido University

60 PUBLICATIONS 670 CITATIONS

[SEE PROFILE](#)



[Hiroshi Hinou](#)

Hokkaido University

76 PUBLICATIONS 1,074 CITATIONS

[SEE PROFILE](#)

Rapid Endolysosomal Escape and Controlled Intracellular Trafficking of Cell Surface Mimetic Quantum-Dots-Anchored Peptides and Glycopeptides

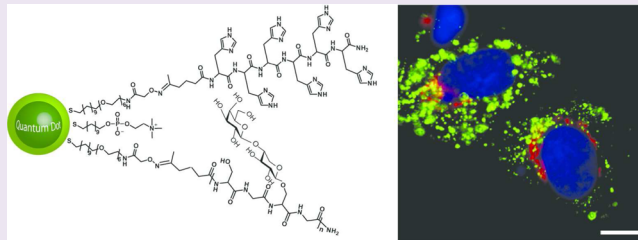
Roger S. Tan,[†] Kentaro Naruchi,[‡] Maho Amano,[†] Hiroshi Hinou,^{†,‡} and Shin-Ichiro Nishimura^{*,†,‡}

[†]Faculty of Advanced Life Science and Graduate School of Life Science, Hokkaido University, N21, W11, Kita-ku, Sapporo 001-0021, Japan

[‡]Medicinal Chemistry Pharmaceuticals Co., Ltd., N21, W12, Kita-ku, Sapporo 001-0021, Japan

S Supporting Information

ABSTRACT: A novel strategy for the development of a high performance nanoparticles platform was established by means of cell surface mimetic quantum-dots (QDs)-anchored peptides/glycopeptides, which was developed as a model system for nanoparticle-based drug delivery (NDD) vehicles with defined functions helping the specific intracellular trafficking after initial endocytosis. In this paper, we proposed a standardized protocol for the preparation of multifunctional QDs that allows for efficient cellular uptake and rapid escaping from the endolysosomal system and subsequent cytoplasmic molecular delivery to the target cellular compartment. Chemoselective ligation of the ketone-functionalized hexahistidine derivative facilitated both efficient endocytic entry and rapid endolysosomal escape of the aminoxy/phosphorylcholine self-assembled monolayer-coated QDs (AO/PCSAM-QDs) to the cytosol in various cell lines such as human normal and cancer cells, while modifications of these QDs with cell-penetrating arginine-rich peptides showed poor cellular uptake and induced self-aggregation of AO/PCSAM-QDs. Combined use of hexahistidylated AO/PCSAM-QDs with serglycine-like glycopeptides, namely synthetic proteoglycan initiators (PGIs), elicited the entry and controlled intracellular trafficking, Golgi localization, and also excretion of these nanoparticles, which suggested that the present approach would provide an ideal platform for the design of high performance NDD systems.



Nanoparticle-based drug delivery (NDD) systems have emerged as a promising approach to enhance the efficacy of existing drugs as well as a new class of potent therapeutic reagents based on the characteristic properties and functions of nanocarriers themselves. The advantage of nanomedicine is evident because NDD vehicles have unique potentials for multifunctionality that allow for displaying multiple discrete compounds such as bioactive molecules (drugs), affinity ligands, and imaging probes within a single nanoparticle platform to achieve molecular targeted and traceable drug delivery to disease sites.^{1–4} However, it is considered that there are still some critical issues to be resolved for achieving an optimal benefit of NDD.^{5–10} The key to its success is the ability to mediate the facile and efficient delivery of the nanoparticles to the cytosol of mammalian cells. It is clear that NDD systems ultimately need to deliver various drugs to the targeted molecules in the intracellular space, not only to the specific/targeted cells but also to various subcellular compartments and organelles.^{11–16}

Quantum dots (QDs) are fluorescent semiconductor nanoparticles that have unique optical properties, including narrow band and size-dependent luminescence with broad absorption, long-term photostability, and resistance to photobleaching. Among an array of potential nanoparticle materials currently used in biology, for example, those made from noble metals,

transition metals, silicon, functionalized polymers, and liposomes,^{17–21} QDs have great potential to be an ideal model system for facilitating systematic monitoring and evaluating all stages of NDD with high sensitivity and high resolution due to their unique intrinsic photophysical characteristics. Therefore, it is evident that QDs have high potential to be an ideal platform for nanocarrier design, since we may have a plethora of choices of methods for the surface modification of QDs to give a required function and property.^{1–4,17–21} However, we have strongly felt the needs of a standard protocol for the preparation of highly functionalized QD surfaces that can efficiently display various ligand molecules without any significant changes in the surface properties after conjugation with ligands. Recently, we reported an efficient and versatile method for the preparation of multifunctional QDs, aminoxy/phosphorylcholine self-assembled monolayer-coated QDs (AO/PCSAM-QDs), that can display covalently with various synthetic glycosides in a quantitative manner with excellent solubility and long-term stability in aqueous solution without the loss of quantum yields.^{22–24} The combined use of an

Received: March 14, 2015

Accepted: June 24, 2015

Published: June 24, 2015



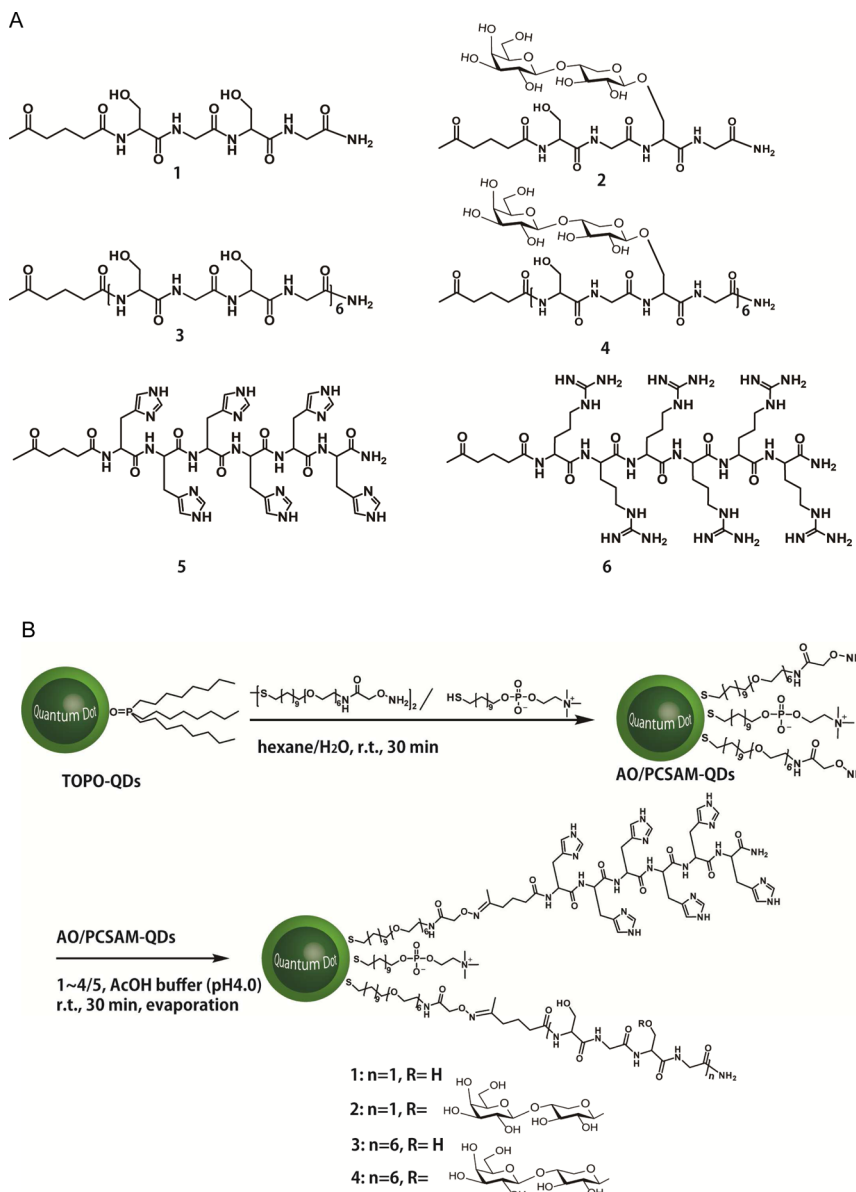


Figure 1. Chemical structures of ketone-functionalized peptides and PGI glycopeptides used in this study (A) and a general protocol for the preparation of AO/PCSAM-QDs ($\text{AO}/\text{PC} = 1/20$) carrying His_6 derivative 5 and compounds 1–4 ($5/1-4 = 1/1$), concurrently (B). Although this scheme shows the preparation of QD conjugates displaying two different peptide components, other QD conjugates carrying single peptide or glycopeptide were also prepared in order to profile individual properties and potentials. For the synthesis, characterization of all new compounds used herein, and detailed conditions for the preparation of QD conjugates, see also the Supporting Information.

aminoxy-terminated monothiol derivative, 11,11'-dithio bis-[undec-11-yl 12-(aminoxyacetyl)amino hexa(ethylene glycol)] (AOSH), and a phosphorylcholine-type monothiol derivative, 11-mercaptopoundecylphosphorylcholine (PCSH), provided QDs with highly versatile functions for the chemical ligation of ketone-functionalized compounds and nonfouling surface characteristics to prevent nonspecific protein adsorption concurrently. A simple, mild, and selective ligation strategy using cell surface mimetic AO/PCSAM-QDs with ketone-functionalized glycosides that was derived from the corresponding simple *p*-nitrophenyl glycosides allowed for the efficient preparation of QDs displaying various oligosaccharides (glyco-PC-QDs) in a quantitative manner. *In vivo* near-infrared (NIR) fluorescence imaging of a variety of glyco-PC-QDs after administration into the tail vein of the mouse has revealed for the first time that our approach can visualize the evidence of

an essential role of the specific glycan structures bearing terminal sialic acid residues for achieving prolonged *in vivo* lifetime and biodistribution of the glycosylated QDs as an ideal glycoprotein model.^{22–24}

It is known that the internalization of QDs exogenously added to cultured cells is caused mostly by nonspecific endocytosis while the mechanism depends strongly on factors such as the QD size, surface coating, stability, hydrodynamic property, concentration, cell type, and the duration of incubation.^{25–28} The combined use of cell penetrating peptides (CPPs)^{29–35} with nanoparticles may be a potential approach to improve the efficacy of cellular uptake of QD conjugates. In fact, it has been documented that endocytosis can be enhanced significantly by modifying the QDs' surface with histidine-tagged arginine-rich CPPs or nuclear localization signal (NLS) peptides.^{36–39} However, it should be noted that internalized

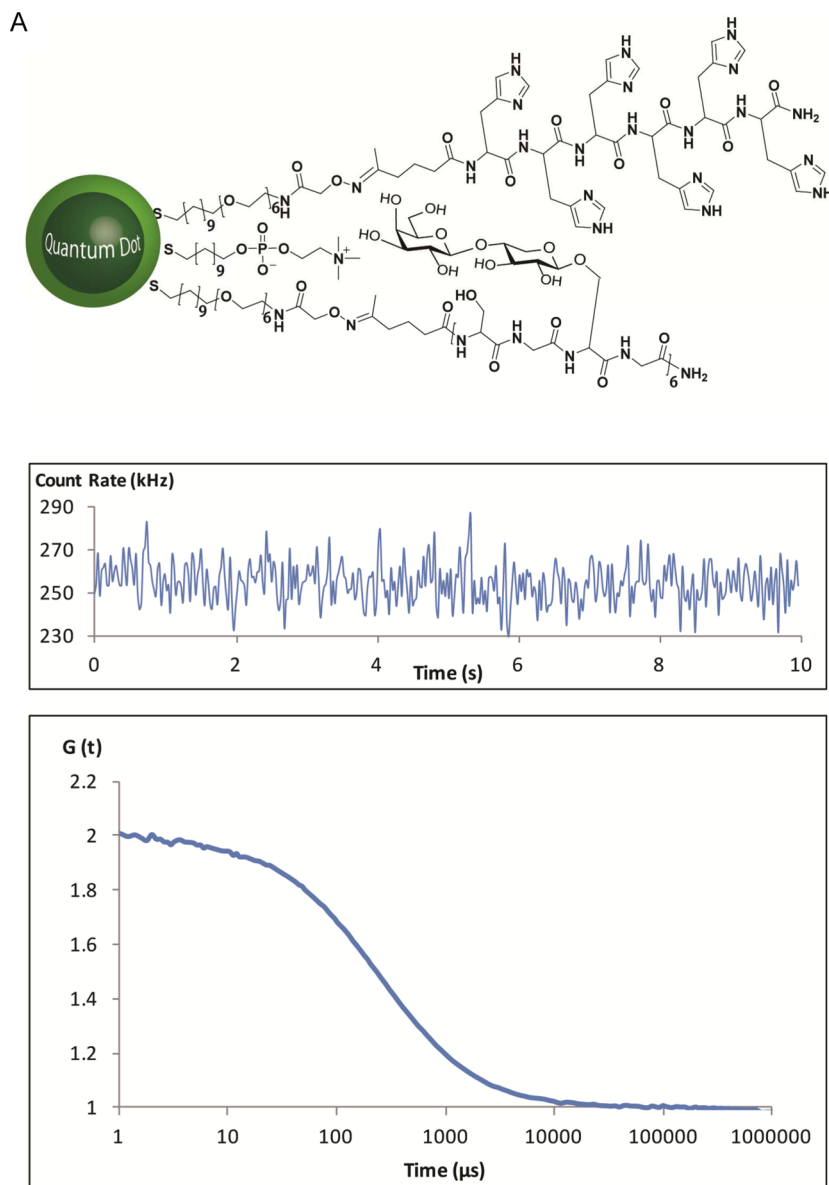


Figure 2. continued

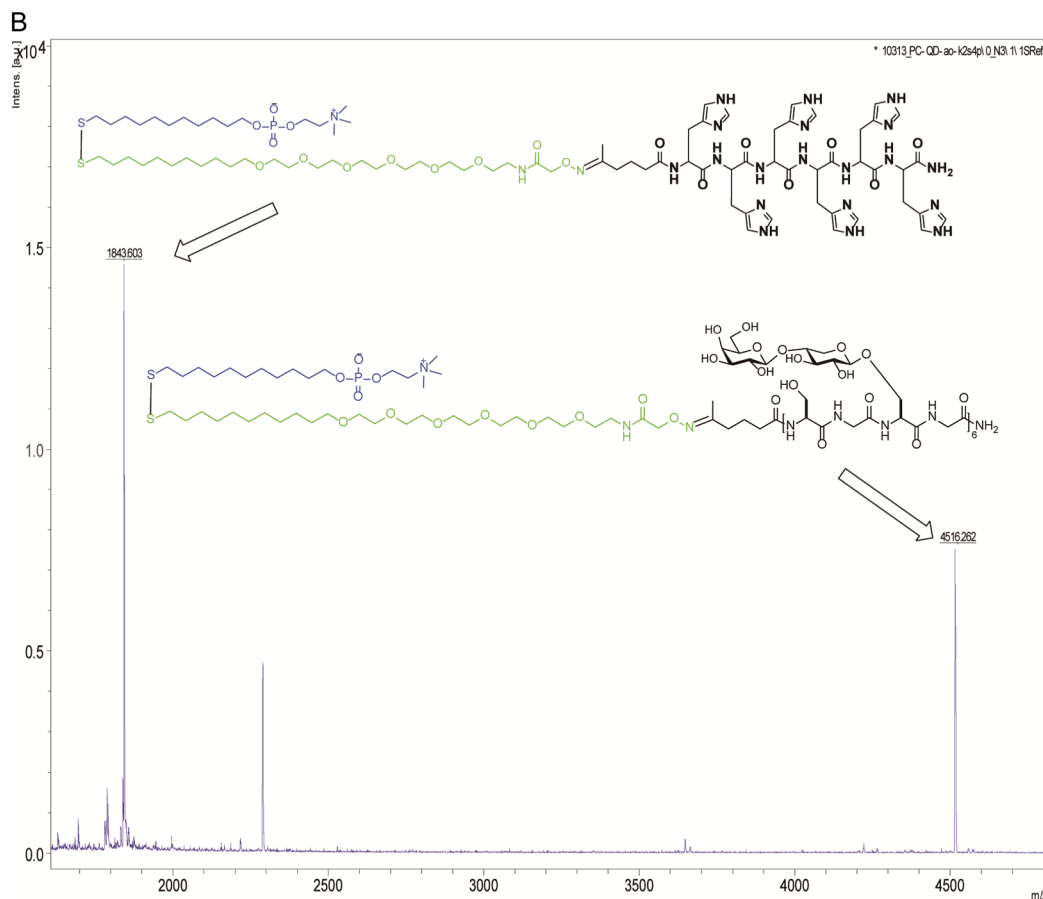


Figure 2. Characterization of AO/PCSAM-QDs (AO/PC = 1/20) carrying His₆ derivative **5** and glycopeptide **4** prepared by the standard protocol. (A) Fluorescence fluctuation in water. The autocorrelation curve was fitted by using one component diffusion model. (B) Heterodimeric ions generated from QD conjugates during direct MALDI-TOFMS measured at positive mode. As for the characterization of AO/PCSAM-QDs carrying His₆ derivative **5** and compounds **1–3**, see Figure S14–16 in the Supporting Information.

QDs are mostly trapped within endosomal compartments, which may block their ability to reach specific intracellular targets.^{5–16} Recently, it has been reported that modification of QDs with palmitoylated histidine-tagged peptide (Palm-1) can facilitate their endosomal escape while the QDs released from endosomes was maximal at 24–48 h postdelivery after incubation with COS-1 and HEK 293T/17 cells.¹⁵ Commercial polymer PULSin also exhibited an ability to assist endosomal escape of QDs when incubated with both cells, though PULSin elicited a considerable degree of cytotoxicity in these cell lines.¹⁵ Further studies on combinatorial and intuitive structure–activity relationship analysis of a variety of peptides (Palm-1 analogs) would allow for selection of multifunctional peptides showing more efficient uptake and endosomal escape of QDs.¹⁶

In the present study, we focus on cellular uptake, intracellular fate, and controlled intracellular delivery of ligands such as peptides and glycopeptides displayed on the cell surface mimetic AO/PCSAM-QDs platform as an ideal model of a multifunctional NDD vehicle. Since the imidazole groups of multiple histidine residues involved in some CPPs and NLS peptides are essential for endosomolytic activity of the peptide/DNA complexes through the protonation in the acidic endosome resulting in the cytoplasmic release of the ligands,^{40–46} we hypothesize that attachment of ketone-functionalized histidine-rich peptides to the surface of the AO/PCSAM-QDs platform carrying various ligands through

direct ligation greatly facilitates endocytosis, endolysosomal escape, and subsequent cytoplasmic delivery of the QD conjugates to the desired intracellular compartment.

RESULTS AND DISCUSSION

Facile and Controlled Display of Peptides/Glycopeptides on Nanoparticles. We have focused on the development of a universal set of tools to attach systematically any peptides and glycopeptides to the surface of AO/PCSAM-QDs in a manner that satisfies some important criteria required for the ideal NDD vehicles such as (a) versatility and reproducibility in the protocol for the surface manipulation and the attachment of ligands, (b) long-term stability of the QD conjugates, (c) controlled orientation and density of the ligands displayed, and (d) biocompatibility required for the live cell and animal imaging.

Figure 1 shows a simple and efficient method for the direct conjugation of ketone-functionalized peptides/glycopeptides **1–4**, synthetic proteoglycan initiators (PGIs) as model ligands targeting Golgi,^{47,48} and hexahistidine (His₆)/hexaarginine (Arg₆) derivatives **5** and **6** with AO/PCSAM-QDs^{22–24} (for detailed experimental conditions of the synthesis of all new compounds **1–6** and characterization data, see Supporting Information). To assess the feasibility of this method as a standardized protocol for the preparation of general peptides–QD conjugates, a variety of QD conjugates were prepared on the basis of this concept using AO/PCSAM-QDs (AO/PC =

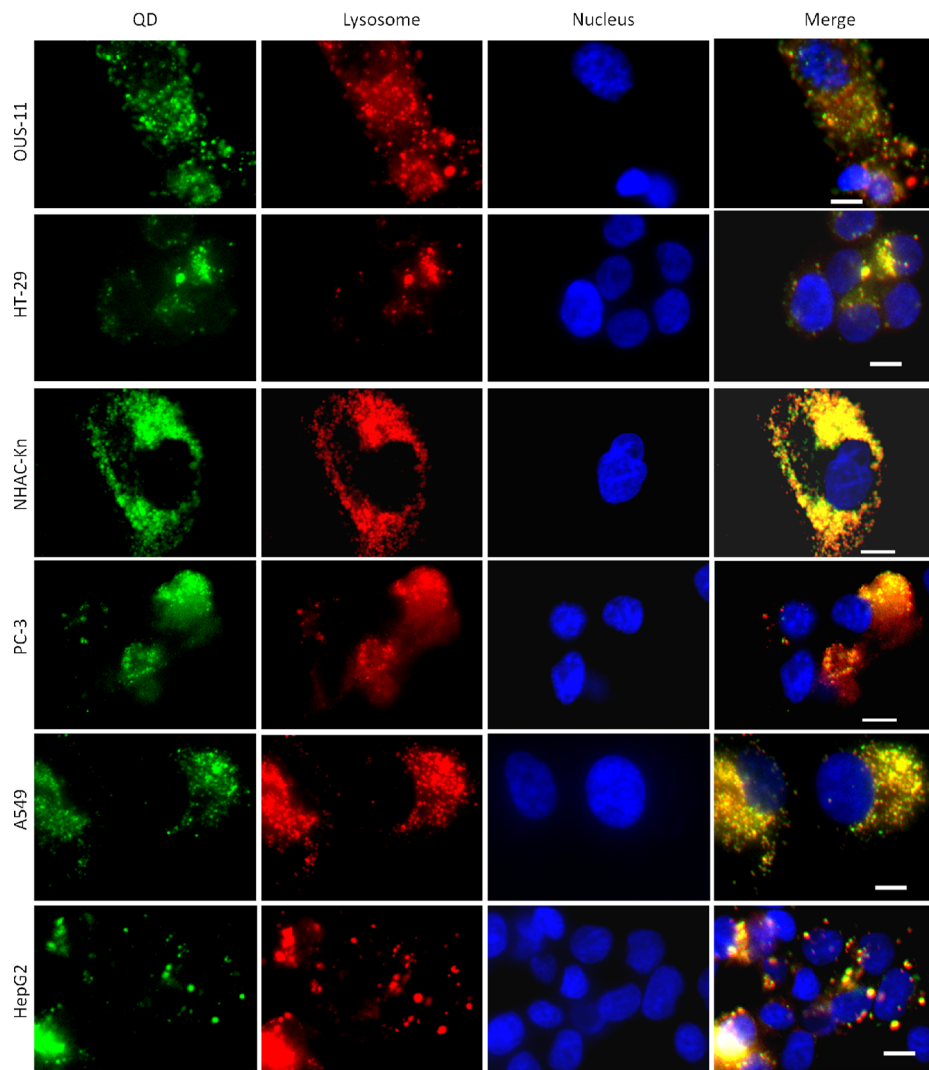


Figure 3. Representative cell images showing lysosomal accumulation of most AO/PCSAM-QDs ($\text{AO}/\text{PC} = 1/20$) carrying serglycine-like PGI glycopeptide **4** after coincubation for 2 h. Scale bar, 10 μm . Cells were coincubated with QD conjugates (green) for 2 h and fixed. Lysosomes were stained with LysoTracker Red DND-99 (red), while the nuclei were stained with Hoechst 33342 (purple). Merged yellow color indicates that the QD conjugates were mostly accumulated and suffered from endolysosomal sequestration after 2 h. AO/PCSAM-QDs ($\text{AO}/\text{PC} = 1/20$) carrying serglycine-like PGI glycopeptide **4** was prepared according to the standard protocol reported previously (see the Supporting Information).^{22–24}

1/20) and synthetic ketone-functionalized peptides/glycopeptides **1–6**, and they were characterized systematically according to the methods reported previously.^{22–24} As a result, the merit of the present protocol for the preparation of multifunctional QD conjugates was evident because (a) a seamless solid-phase peptide/glycopeptide synthesis accelerated under microwave irradiation^{49,50} could be applied efficiently in a straightforward manner toward the preparation of the various targeted ketone-functionalized peptides and glycopeptides by terminating the peptide synthesis with 5-oxohexanoic acid at the *N* terminus,^{51–54} (b) ligation of these ketone-terminated peptides/glycopeptides with aminoxy (AO)-functional groups⁵⁵ displayed on the surface of AO/PCSAM-QDs proceeded smoothly under mild conditions (pH 4.0, 40 °C, and totally 1 h incubation)^{22–24,54,55} without any activating reagent to afford desired QD conjugates in a quantitative yield, in which densities of the attached ligands can be controlled by varying the molar ratio of AOSH and PCSH employed for the preparation of the original AO/PCSAM-QDs platform (in the present study, the molar ratio was fixed as $\text{AO}/\text{PC} = 1/20$), and

(c) AO/PCSAM-QDs carrying various peptides and glycopeptides showed an excellent nonfouling surface property and functionalities required for further *in vitro* investigations such as cellular uptake and subsequent controlled intracellular trafficking experiments. As characterized by fluorescence correlation spectroscopy (FCS), the fluorescence fluctuation of AO/PCSAM-QDs carrying compounds **4** and **5** proved to be rapid and an ideal profile in the fitting curves with a single-component diffusion model (Figure 2A). Direct ionization of ligands on the metal-based nanoparticles^{56,57} under the laser irradiation in MALDI-TOFMS showed clearly that the generation of two major heterodimer ions at *m/z* 1843.6 and *m/z* 4516.3 formed by cross-linking PCSH with oximes derived from AOSH and ketone-functionalized His₆ derivative **5** or glycopeptide **4**, respectively (Figure 2B, see also Figure S14–16 in Supporting Information). Most importantly, there was no ion peak due to compound **5**, indicating clearly that the histidine oligomer did not coordinate directly with the QD metal surface. Multiple histidine derivatives could form noncovalent coordination on the metal surfaces, which could

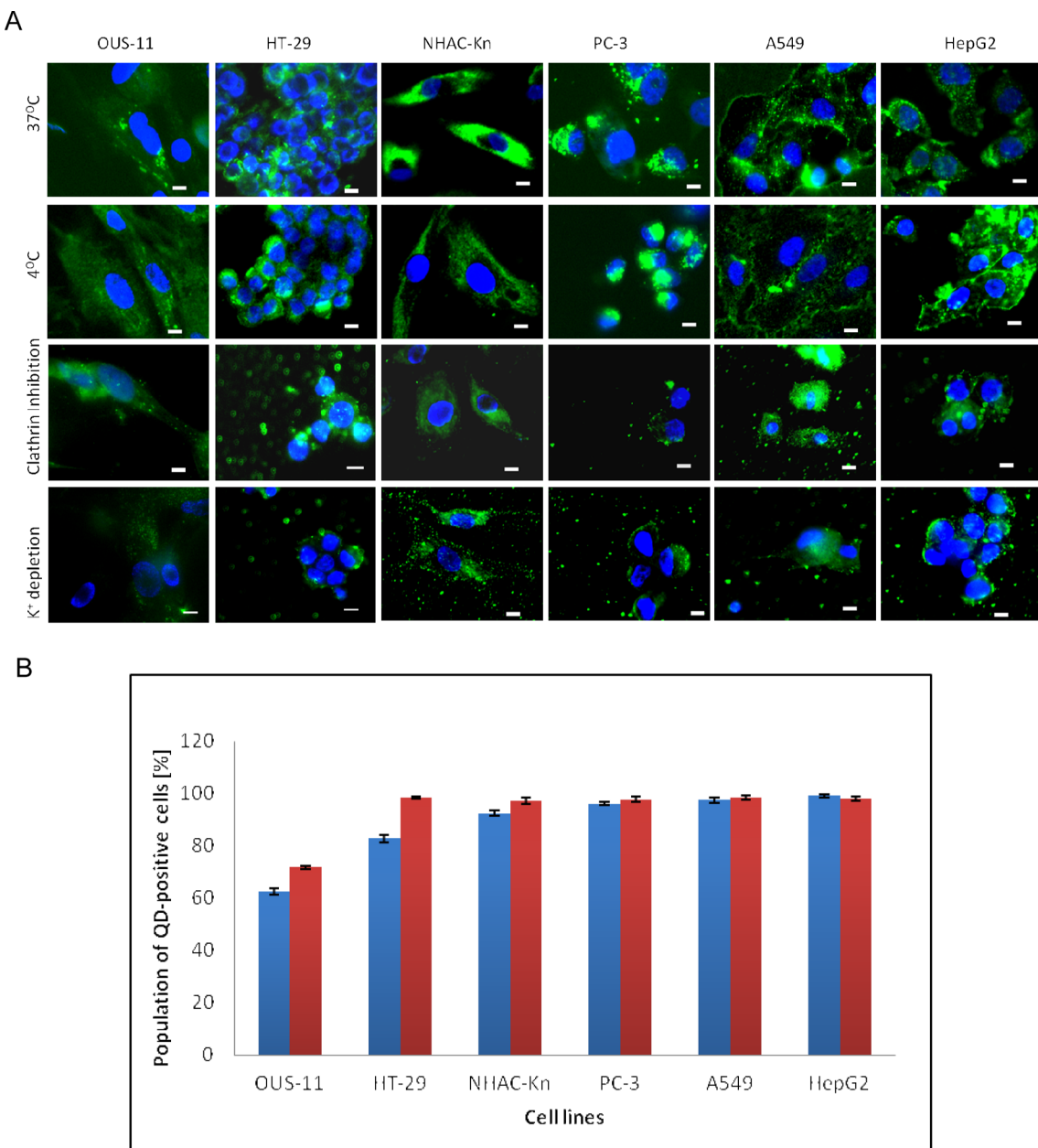


Figure 4. Endocytic incorporation of AO/PCSAM-QDs (AO/PC = 1/20) carrying His₆ derivative **5** (50% of amine-functional groups of the AO/PCSAM-QDs was modified by His₆ derivative **5** using an optimized condition). (A) Representative cell images showing cellular uptake of QDs carrying His₆ derivative **5** (green) at different endocytic inhibition conditions. Nuclei were stained with Hoechst 33342 (purple). Scale bar shows 10 μ m. (B) Effect of the different temperature (red, 37 °C and blue, 4 °C) on the cellular uptake efficiency of QD conjugates carrying His₆ derivative **5**.

also become a nice method for direct QD surface modification.¹⁵ However, during the formation of late endolysosome, it is also known that the pH inside the cells can drop to as low as 5.0–5.5. Given the fact that the normal pK_a of histidine residue was 6.5, protonation of its imidazole side chain could result in the dissociation of histidine oligomers from the QD surface. On the other hand, it should be emphasized that modification of the QD surface with amphiphilic AO-SH and PC-SH linkers that yielded stable SAMs²² could make direct coordination of the imidazole groups of His₆ derivative **5** and the ZnS-based QD surface impossible due to the steric hindrance and lack of an exposed QD surface. In addition, a cell viability test using normal and various cancer cell lines indicated no serious cytotoxicity during

24 h coincubation with all QD conjugates used in this study at a concentration range from 5 to 20 nM (Figure S24 in Supporting Information). These results demonstrated that coating dominantly by self-assembled phosphorylcholine-type linker (PCSH) was essential to providing a nanoparticles surface with a basic cell membrane-like nature found in all of these QD conjugates derived from the AO/PCSAM-QDs platform. Considering the fact that naturally occurring bioactive compounds and small molecular therapeutic reagents as well as peptides/proteins had mostly amino-functional group(s) or equivalent auxiliary that could be converted into the ketone-functionality by general chemical modifications, the versatility and benefits of the present strategy in the construction of a

variety of nanoparticles displaying large-scale compound libraries were clear.

Cellular Uptake and Lysosomal Accumulation of AO/PCSAM-QDs. We examined preliminarily cellular uptake and subsequent intracellular traffic of AO/PCSAM-QDs (AO/PC = 1/20) conjugating simply with serglycine-like PGI glycopeptide 4. Our previous study demonstrated that similar macromolecular PGIs tagged with fluorescein isothiocyanate (FITC) could penetrate slowly into normal human chondrocytes (NHAC-Kn cells) across the cell membrane and localize partly in the intracellular compartments such as Golgi and nuclear spaces when they were coincubated with NHAC-Kn cells for 24–48 h.⁴⁸ These results might suggest that these PGI glycopeptides could penetrate into the cells through the hydrophobic interaction between the aromatic FITC moiety modified at the *N*-terminus of the glycopeptides and cell membranes composed of amphiphatic lipids, as pointed out in cases for many simple PGIs bearing an aromatic moiety at the anomeric position.^{58,59} The PGI glycopeptides displayed on the surface of QDs might be incorporated into the cells based on “endocytosis,” one of the most important and major mechanisms during the cellular uptake of nanoparticles.^{5–16,29–35} We considered that QD conjugates derived from AO/PCSAM-QDs could also be incorporated into the cells by an endocytic mechanism, although they must be trapped immediately by lysosomes and accumulated mostly within endolysosomal compartments. As anticipated, it was revealed that AO/PCSAM-QDs carrying serglycine-like macromolecular glycopeptide 4 were incorporated smoothly and accumulated dominantly in the endolysosomes when they were coincubated with various human cell lines for 2 h (Figure 3). This result strongly suggested the need of an additional functional motif for controlling cellular uptake efficiency and subsequent intracellular trafficking of these QD-based nanoparticle-vehicles.

Endocytosis and Endolysosomal Escape of AO/PCSAM-QDs by Conjugating Hexahistidine Derivative. Our attention was next directed to the unique functions of the multiple histidine peptide moiety^{40–46} during the entry from the extracellular space and subsequent intracellular trafficking of cell surface mimetic QD conjugates, especially the ability to assist subsequent endolysosomal escape of AO/PCSAM-QDs. First we designed and prepared AO/PCSAM-QDs carrying multiple histidine residues, and tested the effect of the introduction of histidine-rich peptide, a ketone-functionalized His₆ derivative 5, on the general property and efficacy of PCSAM-QD platform^{22–24} in the cellular uptake using several human cell lines. As shown in Figure 4A (photos at the top), it was revealed that AO/PCSAM-QDs carrying His₆ derivative 5 [50% of aminoxy-functional groups of the AO/PCSAM-QDs (AO/PC = 1/20) was modified by compound 5 using an optimized condition] were incorporated efficiently after 2 h into all cell lines used herein under a common physiological condition at 37 °C, while efficiency of the uptake appeared to differ significantly between normal (OUS-11) and cancer (AS49) cells (for the optimization of the standard protocol using compound 5, see Figures S18–23 and the experimental section in the Supporting Information).

Cellular internalization of common QD conjugates was supposed to follow nonphagocytic endocytosis in most cells by several recognized mechanisms including clathrin-mediated endocytosis, caveolin-mediated endocytosis, clathrin- and caveolin-independent mechanisms, and actin (ATP/energy)-

dependent micropinocytosis.^{28,60–63} Several of these processes could be working together at the same time within a cell, and therefore, the mechanism of QDs uptake might vary within and between different cell types. To determine the possible uptake pathway and mechanism utilized by the cell surface mimetic QD conjugates, we elucidated cellular uptake of AO/PCSAM-QDs (AO/PC = 1/20) carrying His₆ derivative 5 under different temperatures or different inhibition conditions (Figure 4A). Although the cell incubation at 4 °C resulted in a slight reduction of cellular uptake of QD conjugates by OUS-11, HT-29, and NHAC-Kn cells compared with the normal physiological temperature at 37 °C, lowering the incubation temperature did not affect the uptake efficiency of most cells (Figure 4B). Disruption of the formation of clathrin-coated pits by K⁺ depletion or hypertonic treatment (HT) of cells^{60,61} did not inhibit the cellular uptake of the QD conjugates in all of the cell lines. In addition, HepG2 cells known as a caveolae-deficient cells that did not express caveolins endogenously⁶² also showed a quite similar profile in cellular uptake of the QD conjugates, indicating that QD conjugates internalized into the cells independent from the lipid raft-mediated mechanism. All these results clearly demonstrated that the main endocytic pathway of these QDs was nonspecific physical endocytosis independent from clathrin/caveolin-mediated mechanism, which was notably an energy-independent mechanism that involves direct translocation and induction of endocytic-like membrane invagination leading to endosome-like invaginations without participation of metabolic energy.

On the contrary, it was uncovered that AO/PCSAM-QDs (AO/PC = 1/20) displaying Arg₆ derivative 6 prepared by the standard protocol rapidly formed large aggregates and located mostly on the surface of the cell membrane as well as the extracellular space (Figure S17 in Supporting Information). Generally, it has been considered that polyarginine-conjugated compounds as well as other cell penetrating peptides bearing multiple arginine residues could enter cells through the ionic interaction with cell surface heparin sulfate.^{64,65} However, it was also reported that large vesicles containing arginine-rich Tat peptide-conjugated QDs (QDs carrying arginine-rich peptide, RRRQRRKKRGY) were attached to filopodia or were observed as free structures in the culture medium.³⁷ More importantly, endocytosed Tat peptide-conjugated QDs were also tethered to the vesicular membranes, indicating that arginine-rich Tat peptide had strong affinity with cellular membrane structures.³⁷ These results suggested that multiple guanidino groups of the arginine-rich peptide 6 conjugated with AO/PCSAM-QDs would interact more strongly with phosphorylcholine moiety both of QD surfaces and phosphatidyl choline, which was the most abundant lipid among cell membrane components, while AO/PCSAM-QD conjugates displaying His₆ derivative 5 were efficiently incorporated into the cells tested herein and appeared to distribute dominantly in the cytoplasmic space without significant aggregation (Figure 4A and Figure S17 in the Supporting Information). However, we also demonstrated that aggregation of QD conjugates was observed at a ratio of His₆ derivative 5 higher than 50% with respect to the glycopeptide ligands (Figures 18–23 in the Supporting Information). These results indicated that the efficacy of nonspecific physical endocytosis of the AO/PCSAM-QD conjugates displaying His₆ derivative 5 depended strongly on the general surface nature of these nanoparticles covered largely by self-assembled monolayer of the phosphorylcholine-type linker.⁵ In other words, it seemed that attachment of His₆

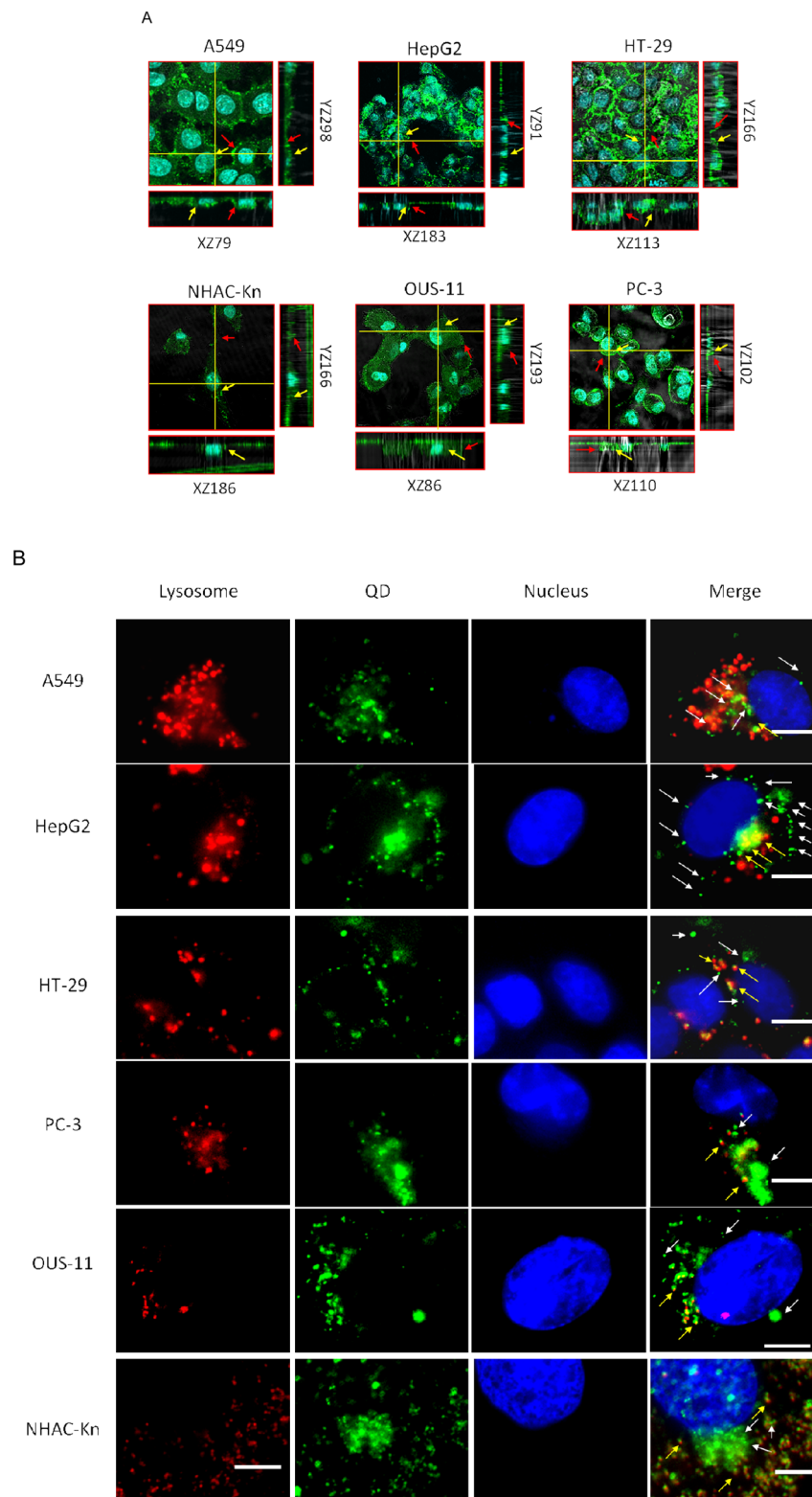


Figure 5. continued

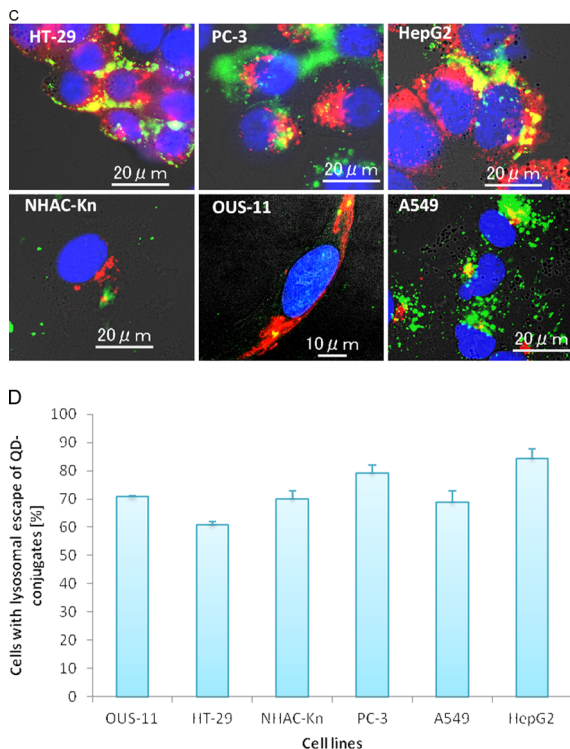


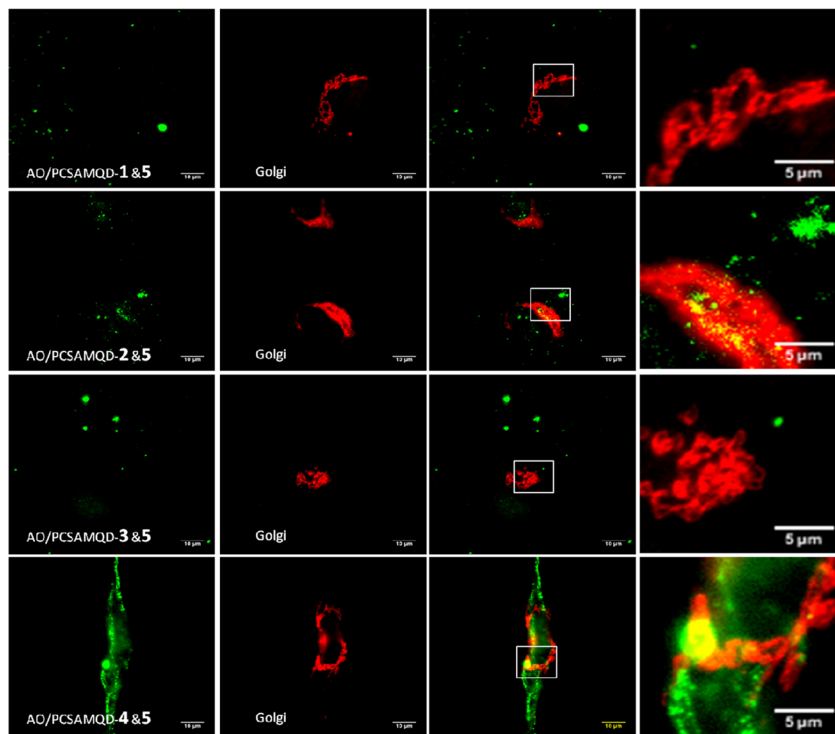
Figure 5. Uptake and controlled intracellular trafficking of AO/PCSAM-QDs ($\text{AO}/\text{PC} = 1/20$) carrying both PGI glycopeptide **4** and His₆ derivative **5** (the ratio of compounds **4** and **5** was fixed as 1:1 by using the standard protocol described in the Experimental Section and Supporting Information). (A) Orthogonal 3D views of different human cell lines coincubated with AO/PCSAM-QDs carrying compounds **4** and **5** at 4°C , showing localization of QD conjugates both in the cytoplasm (pointed by yellow arrows) and plasma membrane (pointed by red arrows). (B) Representative cell images showing intracellular distribution of QD conjugates (green) when coincubated with different human cell lines for 2 h. Lysosomes were stained with Lysotracker Red DND-99 (red) while the nuclei were stained with Hoechst 33342 (purple). White arrows indicate QD conjugates excluded from lysosome. Yellow arrows indicate areas of colocalization uncovered by merged pictures. Scale bar is $10 \mu\text{m}$. (C) Representative images of cells having QD conjugates carrying compounds **4** and **5** colocalized in the Golgi following escaped from endolysosomal entrapment in different human cell lines. Cells were coincubated with QD conjugates (green) for 2 h and fixed. Golgi apparatuses were tagged with antigenin and detected with a secondary antibody (red) while the nuclei were stained with Hoechst 33342 (purple). Merged yellow color indicates that the QD conjugates accumulated in the Golgi after the endolysosomal escape. (D) Semiquantitative scoring of lysosomal escape in the different human cell lines. Error bar represents SEM for $n = 300$ (three scoring trials with 100 cells each trial in random fields). Semiquantitative scoring was done by counting the number of cells having QD conjugates carrying compounds **4** and **5** localized in the Golgi after 2 h of coincubation. The presence of QD conjugates in the Golgi indicated that QD conjugates have successfully escaped from the endolysosomal entrapment.

derivative **5** did not have significant influence on the cellular uptake of AO/PCSAM-QDs displaying peptide/glycopeptide derivatives when the ratio was lower than 50%. It was clear that the difference between AO/PCSAM-QDs displaying His₆ derivative **5** and Arg₆ derivative **6** depended on the pK_a of the imidazole and guanidine groups.

To verify that cell uptake and intracellular traffic of AO/PCSAM-QDs carrying PGI glycopeptides could be mediated specifically by the presence of His₆ derivative **5**, cells were coincubated with AO/PCSAM-QDs ($\text{AO}/\text{PC} = 1/20$) codisplaying glycopeptide **4** and His₆ derivative **5** at 4°C (Figure 5A) and 37°C (Figure 5B). As shown in Figure 5A, Z-track images of the cells clearly showed that QD conjugates carrying both glycopeptide **4** and His₆ derivative **5** distributed both in the cytoplasm and in the plasma membrane. The result indicated that AO/PCSAM-QDs ($\text{AO}/\text{PC} = 1/20$) having both compound **5** and **4** were also incorporated into the cells by energy-independent nonspecific physical endocytosis as observed in that of QD conjugates bearing compound **5** (Figure 4A). It was also uncovered that attachment of the ketone-functionalized His₆ derivative **5** allowed for efficient cellular uptake and subsequent endosomal escaping of the QD conjugates at 37°C after 2 h of incubation of all cell lines had

been tested (Figure 5B). Merged pictures indicated that most QD conjugates elicited an efficient endolysosomal escape from sequestration as clearly shown in an intracellular green fluorescence due to the QD conjugates (pointed by white arrows) that did not overlap with the endolysosomal red fluorescence, while only a limited number of QDs appeared to still localize in the lysosomal compartments detected as overlapped yellow particles (pointed by yellow arrows). On the other hand, when Golgi apparatuses were tagged with antigenin IgG and detected with secondary antibody (red), merged yellow color was detected significantly in all cell lines while the fluorescent intensity might be different between these cell lines (Figure 5C). These results suggested clearly that AO/PCSAM-QDs displaying both serglycine-like glycopeptide **4** and His₆ derivative **5** were being delivered partly into the Golgi apparatus after the rapid escape from endolysosomal sequestration. Golgi localization of these QD conjugates after lysosomal escape was observed in a range from 60% to 85% of the cells employed after 2 h of coincubation (Figure 5D). In addition, the 12 frames selected from the real time imaging video for the first 74 s after coincubation of PC-3 cells in the presence of the QD conjugates clearly showed evidence of the rapid intracellular trafficking of QD conjugates on various

A



B

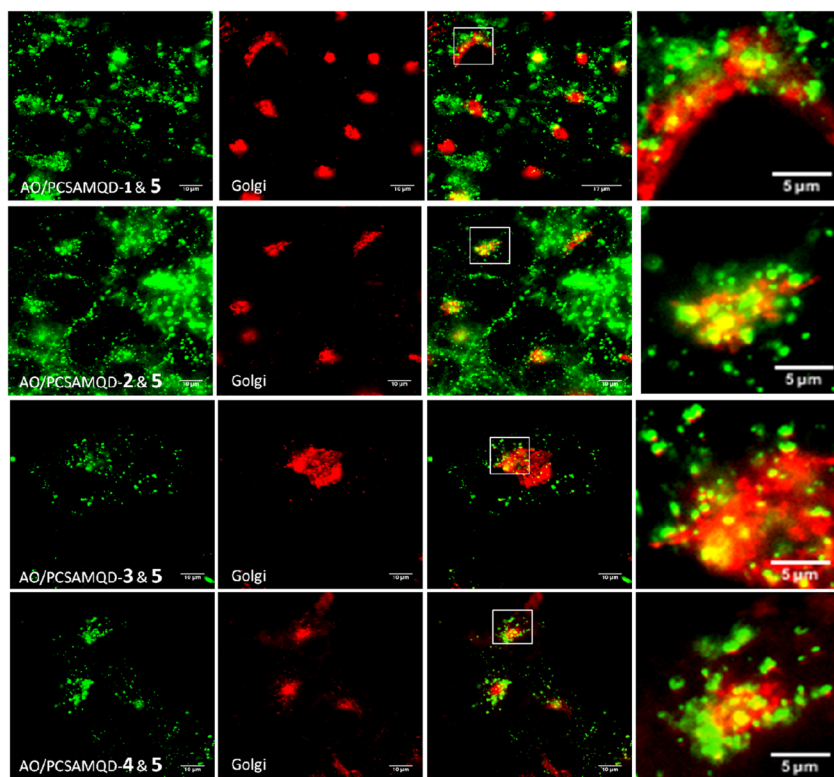


Figure 6. Representative cell images showing controlled intracellular delivery after 2 h of coincubation of human cell lines with 5 nM AO/PCSAM-QDs (AO/PC = 1/20) carrying serglycine-like peptides/glycopeptides **1**, **2**, **3**, and **4** (each 50% of AO-functional groups) in the presence of His₆ derivative **5** (50% of AO-functional groups). Intracellular localization of AO/PCSAM-QDs carrying naked peptides **1** and **3** and glycopeptides **2** and **4** were observed during coincubation with normal human lung tissue (A, OUS-11) and human lung adenocarcinoma (B, A549). Golgi apparatuses were stained by antigen IgG and detected by secondary antibody (goat antimouse IgG H&L-Alexa Fluor647, red). Co-localization was measured using imagej software with plugins: Colocalization Threshold and Colocalization Test by selecting the entire Golgi area inside the region of the interest (ROI).

Table 1. Summary of the Intracellular Distribution of AO/PCSAM-QDs Displaying His₆ Derivative 5 with Compound 1–4^a

compound	OUS-11		HT-29		NHAC-Kn		PC-3		A549		HepG2	
	cytoplasm	Golgi										
1 and 5	+		++	++	+		++	++	+++	++	+++	+++
2 and 5	+	+	++	+	+++	++	++	++	+++	+++	++	+++
3 and 5	+		+++	++	++		+	++	++	++	++	++
4 and 5	+++	++	++	+++	++	+	+	+	+	+	+++	++

^aAll QD conjugates were prepared according to the standard protocol described in the Experimental Section and Supporting Information. As for the representative cell images of HT-29, NHAC-Kn, PC-3, and HepG2, see Figure S25–29 in Supporting Information.

stages from the entry to the excretion processes such as an early endocytic incorporation, first escaped from the endosomal compartment and then delivered to the Golgi apparatus and finally excreted to the area outside the cells (Figure S30 in the Supporting Information). However, since it was likely that the speed of the uptake and intracellular traffic of the QD conjugates appeared to be different between the human cell lines used in the present study, further systematic study might be needed, and the results will be reported in a following communication.

Controlled Golgi Delivery of QD Vehicles Carrying PGI Glycopeptides.

Serglycine-like peptides and glycopeptides 1–4 were supposed to become proteoglycan initiators (substrates) of a series of enzymes, residues of Golgi apparatuses, responsible for the biosynthesis of macromolecular glycosaminoglycans moieties branched from the proximal core peptides.^{47,48} However, it was thought that differences in the structures and molecular size of the compounds 1–4 may greatly influence the profile of the intracellular trafficking of QD conjugates carrying these PGI peptides/glycopeptides, even when all QD conjugates displayed His₆ derivative 5 concurrently. Given that cancer cells generally showed many more activities for both endocytosis of common nanoparticles and biosynthesis of proteoglycans carrying heparan sulfates when compared with normal human cell lines,^{66,67} we hypothesized that the intracellular traffic of the His₆-modified QDs during coincubation with human cancer cells or normal tissue cells could be controlled by the structure of PGI-type ligands 1–4 displayed on these QD conjugates.

As shown in Figure 6, it was revealed that QD conjugates displaying naked peptides 1 or 3 did not localize in the Golgi of normal human lung tissue (OUS-11) while those carrying glycopeptides 2 or 4 appeared to distribute specifically in the Golgi as merged yellow domains. Surprisingly, in the case of human lung adenocarcinoma (A549), all QD conjugates, regardless of molecular size and the presence or absence of glycan moieties, were delivered to the Golgi compartment in a similar manner. This observation exhibited glycan-dependent specific intracellular traffic and localization of the His₆-modified QD conjugates carrying serglycine-like peptides/glycopeptides. It was demonstrated that normal human lung tissue cells could discriminate glycosylated PGI peptides from nonglycosylated serglycine-like peptides while human lung adenocarcinoma could not, although the mechanism has remained unclear. It was noteworthy that a similar glycan-specific localization of His₆-modified QD conjugates was observed in the case of normal human chondrocyte (NHAC-Kn cells) while other cancer cell lines such as HT-29, PC-3, and HepG2 did not show this type of specific Golgi localization of the QD conjugates (Table 1 and Figures S25–29 in the Supporting Information).

Conclusion. We established a standard protocol for the preparation of versatile and multifunctional nanoparticles by means of cell surface mimetic AO/PCSAM-QDs as a key platform for displaying a variety of peptides and glycopeptides. The advantage of the present strategy was evident because this protocol allowed the attachment of general peptides/glycopeptides on the AO/PCSAM-QD surface in a straightforward manner from solid-phase synthesis of ketone tagged peptides/glycopeptides without any special coupling reagents commonly used. It was demonstrated systematically that QD conjugates derived from AO/PCSAM-QDs satisfied some important criteria required for the ideal NDD vehicles such as (a) versatility and reproducibility in the procedure for the surface manipulation and the attachment of ligands having a ketone group or some functionalities that could be conjugated chemoselectively by an aminoxy-functional group, (b) long-term stability of the QD conjugates in solution, (c) controlled orientation and density of the ligands displayed, and (d) biocompatibility needed for the live cell and animal imaging. It should be emphasized that attachment of His₆ derivative 5 was essential for the rapid endolysosomal escape of AO/PCSAM-QD conjugates and intracellular traffic to the cytosol and/or subsequent delivery to the target intracellular compartment in various human cell lines (Figures 4 and 5). Combined use of hexahistidylated AO/PCSAM-QDs with PGI glycopeptides 1–4 elicited dynamic processes of the entry, controlled intracellular trafficking, glycan-specific Golgi localization, and excretion of the nanoparticles from the cytoplasmic area.

Given that many histidine-rich peptides such as CPPs and NLS peptides had been proved to be nice reagents for efficient gene transfer,^{29–35,40–46} it should be noted that the present approach will provide an ideal platform for the design of an entirely novel class of NDD systems targeting specific intracellular compartments. In our previous study, we also revealed that a C-terminal cationic amphipathic peptide (FKIYRKAYQKSLPLLRTIRRWWKK), namely membrane-associated peptide (MAP) found in *Helicobacter pylori* α 1,3/ α 1,4-fucosyltransferases, interacted tightly with cell surface mimetic PCSAM coated magnetic beads and enzymes bearing C-terminal MAP immobilized on the beads function without a significant loss of the biological activities.⁶⁸ Therefore, it was noteworthy that the PCSAM coating strategy might also become a universal tool for highly oriented immobilization of the engineered proteins containing a MAP moiety on the various metal-based nanoparticles.

EXPERIMENTAL SECTION

General procedure for the preparation of AO/PCSAM-QDs.^{22–24} To the 50 μ L of 1 μ M TOPO-QDs from Invitrogen were added isopropanol/methanol (100:50 μ L), which was then centrifuged at 15 000g for 3 min. The solvent was removed, and the pelleted TOPO-QDs were redissolved in 50 μ L of *n*-hexane and

homogenized by sonication. TOPO-QDs/*n*-hexane solution was added with 30 μ L of Milli Q water, 1 μ L of NaBH₄ (12 wt % in 14 N NaOH), 5 μ L of 5 mM 11,11'-dithio bis[undec-11-yl 12-(aminoxyacetyl)amino hexa(ethylene glycol)] (AOSSH) and 10 μ L of 50 mM 11-mercaptopoundecylphosphorylcholine (PCSH). The mixture was mixed for 30 min at RT. The *n*-hexane layer containing TOPO were removed, and washed three times with hexane. The water layer containing AO/PCSAM-QDs was purified using ultra filtration (YM 10) and washed with ultrapure water (400 μ L) three times. The AO/PCSAM-QDs solution was directly analyzed by MALDI-TOFMS (Bruker Daltonics, Bremen, Germany) using DHB (1 μ L, 10 mg mL⁻¹) as a matrix (see also the Supporting Information).

Conjugation of QDs with Ketone-Functionalized Derivatives. To the 10 μ L of AO/PCSAM-QDs solution was added 1 μ L of 10 mM ketone-functionalized peptides/glycopeptides (**1–4**) mixed thoroughly with 1 μ L of 10 mM His₆ derivative **5** (the standard protocol optimized, see also the Supporting Information). The mixture was added with 10 μ L of 200 mM acetate buffer (pH 4.0), mixed for 15–30 min at RT, and concentrated to dryness with a centrifugal evaporator, to complete the oxime formation reaction, for 30 min at 40 °C. The obtained solid was dissolved in Milli Q water, purified using ultra filtration (YM 10), and washed with Milli Q water (400 μ L) three times. The QD conjugates were dissolved in Milli Q water (10 μ L) to obtain a 1 μ M QD solution. The products were directly analyzed by MALDI-TOFMS using DHB (1 μ L, 10 mg mL⁻¹) as a matrix (see also the Supporting Information).

■ ASSOCIATED CONTENT

Supporting Information

Experimental sections for the synthesis and structural characterization of all new compounds, preparation of QD conjugates, characterization of QD conjugates, cell culture, and live cell imaging. The Supporting Information is available free of charge on the ACS Publications website at DOI: 10.1021/acschembio.5b00434.

■ AUTHOR INFORMATION

Corresponding Author

*Phone: +81 11 706 9043. Fax: +81 11 706 9042. E-mail: shin@sci.hokudai.ac.jp.

Notes

The authors declare no competing financial interest.

■ ACKNOWLEDGMENTS

This work was supported by JSPS KAKENHI Grant Number 25220206, JSPS Core-to-Core Program “B. Asia-Africa Science Platform,” and a program “Innovation COE program for future drug discovery and medical care” from the Ministry of Education, Culture, Science, and Technology, Japan. We thank M. Kinjo and A. Kitamura of Faculty of Advanced Life Science, Hokkaido University for the valuable discussion and technical assistances on the characterization of QDs by using FCS.

■ REFERENCES

- (1) Smith, A., Duan, H., Mohs, A., and Nie, S. (2008) Bioconjugated quantum dots for *in vivo* molecular and cellular imaging. *Adv. Drug Delivery Rev.* **60**, 1226–1240.
- (2) Broaders, K. E., Cohen, J. A., Beaudette, T. T., Bachelder, E. M., and Frechet, J. M. J. (2009) *Proc. Natl. Acad. Sci. U.S.A.* **106**, 5497–5502.
- (3) Jain, R. K., and Stylianopoulos, T. (2010) Delivering nanomedicine to solid tumors. *Nat. Rev. Clin. Oncol.* **7**, 653–664.
- (4) Wang, A. Z., Langer, R., and Farokhzad, O. C. (2012) Nanoparticle delivery of cancer drugs. *Annu. Rev. Med.* **63**, 185–198.
- (5) Derfus, A. M., Chan, W. C. W., and Bhatia, S. N. (2004) Intracellular delivery of quantum dots for live cell labeling and organelle tracking. *Adv. Mater.* **16**, 961–966.
- (6) Chen, F., and Gerion, D. (2004) Fluorescent CdSe/ZnS nanocrystal-peptide conjugates for long-term, nontoxic imaging and nuclear targeting in living cells. *Nano Lett.* **4**, 1827–1832.
- (7) Medintz, I. (2006) Universal tools for biomolecular attachment to surfaces. *Nat. Mater.* **5**, 842.
- (8) Chang, Y.-P., Pinaud, F., Antelman, J., and Weiss, S. (2008) Tracking bio-molecules in live cells using quantum dots. *J. Biophoton.* **1**, 287–298.
- (9) Tekle, C., van Deurs, B., Sandvig, K., and Iversen, T.-G. (2008) Cellular trafficking of quantum dot-ligand bioconjugates and their induction of changes in normal routing of unconjugated ligands. *Nano Lett.* **8**, 1858–1865.
- (10) Delehanty, J. B., Matoussi, H., and Medintz, I. L. (2009) Delivering quantum dots into cells: strategies, progress and remaining issues. *Anal. Bioanal. Chem.* **393**, 1091–1105.
- (11) Groc, L., Lafourcade, M., Heine, M., Renner, M., Racine, V., Sibarita, J.-B., Lounis, B., Choquet, D., and Cognet, L. (2007) Surface trafficking of neurotransmitter receptor: Comparison between single-molecule/quantum dot strategies. *J. Neurosci.* **27**, 12433–12437.
- (12) Pinaud, F., Clarke, S., Sittner, A., and Dahan, M. (2010) Probing cellular events, one quantum dot at a time. *Nat. Methods* **7**, 275–285.
- (13) Rajendran, L., Knolker, H.-J., and Simons, K. (2010) Subcellular targeting strategies for drug design and delivery. *Nat. Rev. Drug Discovery* **9**, 29–42.
- (14) Delehanty, J. B., Boeneman, K., Bradburne, C. E., Robertson, K., and Medintz, I. L. (2009) Quantum dots: A powerful tool for understanding the intricacies of nanoparticle-mediated drug delivery. *Expert Opin. Drug Delivery* **6**, 1091–1112.
- (15) Delehanty, J. B., Bradburne, C. E., Boeneman, K., Susumu, K., Farrell, D., Mei, B. C., Blanco-Canosa, J. B., Dawson, G., Dawson, P. E., Matoussi, H., and Medintz, I. L. (2010) Delivering quantum dot-peptide bioconjugates to the cellular cytosol: escaping from the endolysosomal system. *Integr. Biol.* **2**, 265–277.
- (16) Boeneman, K., Delehanty, J. B., Blanco-Canosa, J. B., Susumu, K., Stewart, M. H., Oh, E., Huston, A. L., Dawson, G., Ingale, S., Walters, R., Domowicz, M., Deschamps, J. R., Algar, W. R., DiMaggio, S., Manotno, J., Spillmann, C. M., Thompson, D., Jennings, T. L., Dawson, P. E., and Medintz, I. L. (2013) Selecting improved peptidyl motifs for cytosolic delivery of disparate protein and nanoparticle materials. *ACS Nano* **7**, 3778–3796.
- (17) Medintz, I. L., Uyeda, T. H., Goldman, E. R., and Matoussi, H. (2005) Quantum dot bioconjugates for imaging, labeling and sensing. *Nat. Mater.* **4**, 435–446.
- (18) Kroemer, G., and Jaattela, M. (2005) Lysosomes and autophagy in cell death control. *Nat. Rev. Cancer* **5**, 886–897.
- (19) Beaudette, T. T., Cohen, J. A., Bachelder, E. M., Broaders, K. E., Cohen, J. L., Engleman, E. G., and Frechet, J. M. (2009) Chemoselective ligation in the functionalization. *J. Am. Chem. Soc.* **131**, 10360–10361.
- (20) Susumu, K., Oh, E., Delehanty, J. B., Blanco-Canosa, J. B., Johnson, B. J., Jain, V., Harvey, J., IV, Algar, W. R., Boeneman, K., Dawson, P. E., and Medintz, I. L. (2011) Multifunctional compact zwitterionic ligands for preparing robust biocompatible semiconductor quantum dots and gold nanoparticles. *J. Am. Chem. Soc.* **133**, 9480–9496.
- (21) Algar, W. R., Prasuhn, D. E., Stewart, M. H., Jennings, T. L., Blanco-Canosa, J. B., Dawson, P. E., and Medintz, I. L. (2011) The controlled display of biomolecules on nanoparticles: A challenge suited to bioorthogonal chemistry. *Bioconjugate Chem.* **22**, 825–858.
- (22) Ohyanagi, T., Nagahori, N., Shimawaki, K., Hinou, H., Yamashita, T., Sasaki, A., Jin, T., Iwanaga, T., Kinjo, M., and Nishimura, S.-I. (2011) Importance of sialic acid residues illuminated by live animal imaging using phosphorylcholine self-assembled monolayer-coated quantum dots. *J. Am. Chem. Soc.* **133**, 12507–12517.

- (23) Nishimura, S.-I. (2012) Phosphorylcholine self-assembled monolayers-coated quantum dots: Real-time imaging of live animals by cell surface mimetic glyco-nanoparticles. *Clinics Lab. Med.* 32, 73–87.
- (24) Amano, M., Hinou, H., Miyoshi, E., and Nishimura, S.-I. (2014) Potential usage for in vivo lectin screening in live animals utilizing cell surface mimetic glyco-nanoparticles, phosphorylcholine-coated quantum dots (PC-QDs). *Methods Mol. Biol.* 1200, 361–369.
- (25) Chan, W. C. W., and Nie, S. (1998) Quantum dot bioconjugates for ultrasensitive nonisotopic detection. *Science* 281, 2016–2018.
- (26) Jaiswal, J. K., Mattossi, H., Mauro, J. M., and Simon, S. M. (2003) Long-term multiple color imaging of live cells using quantum dot bioconjugates. *Nat. Biotechnol.* 21, 47–51.
- (27) Pons, T., Uyeda, H. T., Medintz, I. L., and Mattossi, H. (2006) Hydrodynamic dimensions, electrophoretic mobility and stability of hydrophilic quantum dots. *J. Phys. Chem. B* 110, 20308–20316.
- (28) Probst, C. E., Zrazhevskiy, P., Bagalkot, V., and Gao, X. (2013) Quantum dots as a platform for nanoparticle drug delivery vehicle design. *Adv. Drug Delivery Rev.* 65, 703–718.
- (29) Zorko, M., and Langel, U. (2005) Cell-penetrating peptides: Mechanism and kinetics of cargo delivery. *Adv. Drug Delivery Rev.* 57, 529–545.
- (30) Brooks, H., Lebleu, B., and Vives, E. (2005) Tat peptide-mediated cellular delivery: Back to basis. *Adv. Drug Delivery Rev.* 57, 559–577.
- (31) Gupta, B., Levchenko, T. S., and Torchilin, V. P. (2005) Intracellular delivery of large molecules and small particles by cell-penetrating proteins and peptides. *Adv. Drug Delivery Rev.* 57, 637–651.
- (32) Stewart, K. M., Horton, K. L., and Kelley, S. O. (2008) Cell-penetrating peptides as delivery vehicles for biology and medicine. *Org. Biomol. Chem.* 6, 2242–2255.
- (33) Alves, I. D., Bechara, C., Walrant, A., Zaltsman, Y., Jiao, C. Y., and Sagan, S. (2011) Relationships between membrane binding, affinity and cell internalization efficacy of a cell-penetrating peptide: penetration as a case study. *PLoS One* 6, e24096.
- (34) Nakase, I., Akita, H., Kogure, K., Graslund, A., Langel, U., Harashima, H., and Futaki, S. (2012) Efficient intracellular delivery of nucleic acid pharmaceuticals using cell-penetrating peptides. *Acc. Chem. Res.* 45, 1132–1139.
- (35) Gopal, V. (2013) Bioinspired peptides as versatile nucleic acid delivery platforms. *J. Controlled Release* 167, 323–332.
- (36) Delehantry, J. B., Medintz, I. L., Pons, T., Brunel, F. M., Dawson, P. E., and Mattossi, H. (2006) Self-assembled quantum dot-peptide bioconjugates for selective intracellular delivery. *Bioconjugate Chem.* 17, 920–927.
- (37) Ruan, G., Agrawal, A., Marcus, A. I., and Nie, S. (2007) Imaging and tracking of Tat peptide-conjugated quantum dots in living cells: New insights into nanoparticle uptake, intracellular transport, and vesicle shedding. *J. Am. Chem. Soc.* 129, 14759–14766.
- (38) Chen, B., Liu, Q., Zhang, Y., Xu, L., and Fang, X. (2008) Transmembrane delivery of the cell-penetrating peptide conjugated semiconductor quantum dots. *Langmuir* 24, 11866–11871.
- (39) Dawson, P. E., and Mattossi, H. (2008) Intracellular delivery of quantum dot-protein cargos mediated by cell penetrating peptides. *Bioconjugate Chem.* 19, 1785–1795.
- (40) Midoux, P., Kichler, A., Boutin, V., Maurizot, J. C., and Monsigny, M. (1998) Membrane permeabilization and efficient gene transfer by a peptide containing several histidines. *Bioconjugate Chem.* 9, 260–267.
- (41) Mahat, R. J., Monera, O. D., Smith, L. C., and Rolland, A. (1999) Peptide-based gene delivery. *Curr. Opin. Mol. Ther.* 1, 226–243.
- (42) Pichon, C., Goncalves, C., and Midoux, P. (2001) Histidine-rich peptides and polymers for nucleic acids delivery. *Adv. Drug Delivery Rev.* 53, 75–94.
- (43) Kumar, W., Pichon, C., Refrregiers, M., Guerin, B., Midoux, P., and Chaudhuri, A. (2003) Single histidine residue in head-group region is sufficient to impart remarkable gene transfection properties to cationic lipids: Evidence for histidine-mediated membrane fusion at acidic pH. *Gene Ther.* 10, 1206–1215.
- (44) Alexis, F., Lo, S.-L., and Wang, S. (2006) Covalent attachment of low molecular weight poly(ethylene imine) improves Tat peptide mediated gene delivery. *Adv. Mater.* 18, 2174–2178.
- (45) Kichler, A., Leborgne, C., Danos, O., and Bechinger, B. (2007) Characterization of the gene transfer process mediated by histidine-rich peptides. *J. Mol. Med.* 85, 191–201.
- (46) Lo, S.-L., and Wang, S. (2008) An endosomolytic Tat peptide produced by incorporation of histidine and cysteine residues as a nonviral vector for DNA transfection. *Biomaterials* 29, 2408–2414.
- (47) Shimawaki, K., Fujisawa, Y., Sato, F., Fujitani, N., Kuroguchi, M., Hoshi, H., Hinou, H., and Nishimura, S.-I. (2007) Highly efficient and versatile synthesis of proteoglycan core structures from 1,6-anhydro- β -lactose as a key starting material. *Angew. Chem., Int. Ed.* 46, 3074–3079.
- (48) Hoshi, H., Shimawaki, K., Takegawa, Y., Ohyanagi, T., Amano, M., Hinou, H., and Nishimura, S.-I. (2012) Molecular shuttle between extracellular and cytoplasmic space allows for monitoring of GAG biosynthesis in human articular chondrocytes. *Biochim. Biophys. Acta* 1820, 1391–1398.
- (49) Matsushita, T., Hinou, H., Kuroguchi, M., Shimizu, H., and Nishimura, S.-I. (2005) Rapid microwave-assisted solid-phase glycopeptide synthesis. *Org. Lett.* 7, 877–880.
- (50) Garcia-Martin, F., Hinou, H., Matsushita, T., Hayakawa, S., and Nishimura, S.-I. (2012) An efficient protocol for the solid-phase synthesis of glycopeptides under microwave irradiation. *Org. Biomol. Chem.* 10, 1612–1617.
- (51) Fumoto, M., Hinou, H., Ohta, T., Ito, T., Yamada, K., Takimoto, A., Kondo, H., Shimizu, H., Inazu, T., Nakahara, Y., and Nishimura, S.-I. (2005) Combinatorial synthesis of MUC1 glycopeptides: Polymer blotting facilitates chemical and enzymatic synthesis of highly complicated mucin glycopeptides. *J. Am. Chem. Soc.* 127, 11804–11818.
- (52) Fumoto, M., Hinou, H., Matsushita, T., Kuroguchi, M., Ohta, T., Ito, T., Yamada, K., Takimoto, A., Kondo, H., Inazu, T., and Nishimura, S.-I. (2005) Molecular transfer between polymer platforms: Highly efficient chemoenzymatic glycopeptide synthesis by the combined use of solid-phase and water-soluble polymer supports. *Angew. Chem., Int. Ed.* 44, 2534–2537.
- (53) Matsushita, T., Nagashima, I., Fumoto, M., Ohta, T., Yamada, K., Shimizu, H., Hinou, H., Naruchi, K., Ito, T., Kondo, H., and Nishimura, S.-I. (2010) Artificial Golgi apparatus: Globular protein-like dendrimer facilitates fully automated enzymatic glycan synthesis. *J. Am. Chem. Soc.* 132, 16651–16656.
- (54) Matsushita, T., Takada, W., Igarashi, K., Naruchi, K., Miyoshi, R., Garcia-Martin, F., Amano, M., Hinou, H., and Nishimura, S.-I. (2014) A straightforward protocol for the preparation of high performance microarray displaying synthetic MUC1 glycopeptides. *Biochim. Biophys. Acta* 1840, 1105–1116.
- (55) Nishimura, S.-I., Niikura, K., Kuroguchi, M., Matsushita, T., Fumoto, M., Hinou, H., Kamitani, R., Nakagawa, H., Deguchi, K., Miura, N., Monde, K., and Kondo, H. (2005) High throughput protein glycomics: Combined use of chemoselective glycolabelling and MALDI-TOF/TOF mass spectroscopy. *Angew. Chem., Int. Ed.* 44, 91–96.
- (56) Nagahori, N., and Nishimura, S.-I. (2006) Direct and efficient monitoring of glycosyltransferase reactions on gold colloidal nanoparticles by mass spectroscopy. *Chem.—Eur. J.* 12, 6478–6485.
- (57) Nagahori, N., Abe, M., and Nishimura, S.-I. (2009) Structural and functional glycosphingolipidomics by glycolabelling with an aminoxy-functionalized gold nanoparticle. *Biochemistry* 48, 583–594.
- (58) Okayama, M., Kimura, K., and Suzuki, S. (1973) The influence of *p*-nitrophenyl β -D-xyloside on the synthesis of proteochondroitin sulfate by slices of embryonic chick cartilage. *J. Biochem.* 74, 1069–1073.
- (59) Fritz, T. A., Lugenwa, F. N., Sarker, A. K., and Esko, J. D. (1994) Biosynthesis of heparin sulfate on β -D-xylosides depends on aglycone structure. *J. Biol. Chem.* 269, 300–307.

- (60) Puri, V., Watanabe, R., Singh, R. D., Dominguez, M., Brown, J. C., Wheatley, C. L., Marks, D. L., and Pagano, R. E. (2001) Clathrin-dependent and -independent internalization of plasma membrane sphingolipids initiates two Golgi targeting pathways. *J. Cell Biol.* 154, 535–547.
- (61) Kam, N. W. S., Liu, Z., and Dai, H. (2006) Carbon nanotubes as intracellular transporters for proteins and DNA: An investigation of the uptake mechanism and pathway. *Angew. Chem., Int. Ed.* 45, 577–581.
- (62) Rinne, J., Albaran, B., Jylhävä, J., Ihälainen, T. O., Kankaanpää, P., Hytönen, V. P., Stayton, P. S., Kulomaa, M. S., and Vihtinen-Ranta, M. (2007) Internalization of novel non-viral vector TAT-streptavidin into human cells. *BMC Biotechnol.* 7, 1–14.
- (63) Maniti, O., Blanchard, E., Trugnan, G., Lamaziére, A., and Ayala-Sanmartin, J. (2012) Metabolic energy-independent mechanism of internalization for the cell penetrating peptide penetratin. *Int. J. Biochem. Cell B* 44, 869–875.
- (64) Fuchs, S. M., and Raines, R. T. (2004) Pathway for polyarginine entry into mammalian cells. *Biochemistry* 43, 2438–2444.
- (65) Goncalves, E., Kitas, E., and Seeling, J. (2005) Binding of oligoarginine to membrane lipids and heparin sulfate: Structural and thermodynamic characterization of a cell-penetrating peptide. *Biochemistry* 44, 2692–2702.
- (66) Fuster, M. M., and Esko, J. D. (2005) The sweet and sour of cancer: glycans as novel therapeutic targets. *Nat. Rev. Cancer* 5, 526–542.
- (67) Bishop, J. R., Schuksz, M., and Esko, J. D. (2007) Heparan sulphate proteoglycans fine-tune mammalian physiology. *Nature* 446, 1030–11037.
- (68) Naruchi, K., and Nishimura, S.-I. (2011) Membrane-bound stable glycosyltransferases: Highly oriented protein immobilization by a C-terminal cationic amphipathic peptide. *Angew. Chem., Int. Ed.* 50, 1328–1331.